




Cite this: *Lab Chip*, 2018, 18, 1767

A universal platform for selection and high-resolution phenotypic screening of bacterial mutants using the nanowell slide†

H. Antypas,^a M. Veses-Garcia,^a E. Weibull,^{‡b}
H. Andersson-Svahn^b and A. Richter-Dahlfors^b  ^{★a}

The Petri dish and microtiter plate are the golden standard for selection and screening of bacteria in microbiological research. To improve on the limited resolution and throughput of these methods, we developed a universal, user-friendly platform for selection and high-resolution phenotypic screening based on the nanowell slide. This miniaturized platform has an optimal ratio between throughput and assay complexity, holding 672 nanowells of 500 nl each. As monoclonality is essential in bacterial genetics, we used FACS to inoculate each nanowell with a single bacterium in 15 min. We further extended the protocol to select and sort only bacteria of interest from a mixed culture. We demonstrated this by isolating single transposon mutants generated by a custom-made transposon with dual selection for GFP fluorescence and kanamycin resistance. Optical compatibility of the nanowell slide enabled phenotypic screening of sorted mutants by spectrophotometric recording during incubation. By processing the absorbance data with our custom algorithm, a phenotypic screen for growth-associated mutations was performed. Alternatively, by processing fluorescence data, we detected metabolism-associated mutations, exemplified by a screen for β -galactosidase activity. Besides spectrophotometry, optical compatibility enabled us to perform microscopic analysis directly in the nanowells to screen for mutants with altered morphologies. Despite the miniaturized format, easy transition from nano- to macroscale cultures allowed retrieval of bacterial mutants for downstream genetic analysis, demonstrated here by a cloning-free single-primer PCR protocol. Taken together, our FACS-linked nanowell slide replaces manual selection of mutants on agar plates, and enables combined selection and phenotypic screening in a one-step process. The versatility of the nanowell slide, and the modular workflow built on mainstream technologies, makes our universal platform widely applicable in microbiological research.

Received 15th February 2018,
Accepted 7th May 2018

DOI: 10.1039/c8lc00190a

rsc.li/loc

Introduction

Development of the Petri dish, containing nutrient agar for bacterial cultivation, revolutionized the way bacteriologists performed their studies back in the 1880s.^{1,2} Over a century later, it still remains the golden standard to culture, select and screen bacteria to identify new genotypes and phenotypes.³ The large amount of genomic data generated by modern technologies requires, however, high resolution and throughput phenotypic analysis to understand the function of novel genes identified.⁴ This is not easily achieved by agar plate-based methods due to their inherent limitation in phe-

notypic resolution. On agar plates, bacterial growth is usually observed on the macroscale at the incubation endpoint. This restricts the analysis to the measurement of composite growth and disregards individual growth parameters that may be affected by gene mutations, such as growth rate, growth lag, and growth efficiency.^{5–7} Moreover, while agar plate screening is well-suited for qualitative pre-screening of catalytic activity using chromogenic or fluorogenic substrates, quantification is difficult to achieve because of incompatibility between agar plate-based and spectrophotometric methods.⁸ Introduction of time-lapse imaging of colonies growing on solid media, combined with computational analysis can increase the phenotypic resolution.⁹ Still, the sensitivity of such an approach is limited, because bacteria must grow to a considerable number before imaging can capture them on the macroscale. In addition, variations in solid media thickness, agar plate margins, but also nutrient and secreted molecule exchange between neighboring non-individually confined colonies, can lead to spatial bias during phenotypic analysis.⁹

^a Swedish Medical Nanoscience Center, Department of Neuroscience, Karolinska Institutet, Stockholm, Sweden. E-mail: agneta.richter.dahlfors@ki.se

^b Division of Proteomics and Nanobiotechnology, Science for Life Laboratory, KTH-Royal Institute of Technology, Stockholm, Sweden

† Electronic supplementary information (ESI) available. See DOI: 10.1039/c8lc00190a

‡ Current address: Vironova AB, Gävlegatan 22, 113 30 Stockholm, Sweden.



Platforms that use liquid media have a higher throughput and address some of the phenotypic screening limitations encountered on agar plates. The microtiter plate enables kinetic optical recordings and therefore accurate measurement of absorbance and fluorescence to monitor growth and biochemical reactions.¹⁰ The individual components of growth can be analysed and alterations can be identified. Despite these advantages, the well size of commonly used microtiter plates, such as the 96- and 384-well plate, is far from optimal for single-cell analysis.¹¹ Moreover, manual handling of 384-plates can be time-consuming and automated liquid handling may be required for a smooth workflow. Miniaturization of these platforms has enabled high-throughput screening of bacteria on a single-cell level.¹² One such example is the nanowell slide (nwSlide). This platform offers several advantages for microbiological applications compared with commonly used microtiter plates (Table S1, see Note S1†). The nwSlide features 672 wells holding 500 nl each within the dimensions of a microscopy slide.¹¹ Each nanowell acts as an independent container that sustains long-term culturing and analysis of mammalian and bacterial cells.^{13–15}

Here, we leverage the versatile features of the nwSlide to develop a platform for high-resolution phenotypic and genotypic analysis of bacterial mutants (Fig. 1). By integrating fluorescence-activated cell sorting (FACS), kinetic spectrophotometry, optical signal processing and microscopy on the same platform, we were able to screen bacterial mutants based on their growth and metabolic profile, as well as morphotype. Importantly, we established a recovery protocol to transfer selected mutants from nano- to macroscale cultures, and to perform genotyping screening to rapidly map the mutations.

Experimental

Materials

Enzymes were purchased from New England Biolabs (USA), and antibiotics and chemical reagents from Sigma Aldrich

(USA), unless otherwise stated. Primers were synthesized by Eurofins Genomics (Germany) and used in all PCR reactions at a concentration of 10 pmol μL^{-1} . Their sequences and PCR cycling parameters are presented in Table S2 and S3† respectively.

Nanowell slide design and microfabrication

The nwSlide comprises a nanowell-etched silicon grid ($75 \times 0.5 \times 25$ mm) with tapered sides anodically bonded to a borofloat glass wafer ($75 \times 0.175 \times 25$ mm). This bonding results in a 14-column by a 48-row matrix of 672 wells, with center-to-center distance between 2 nanowells at 1500 μm and a volume capacity of 500 nl per nanowell. Due to the outward-tilted walls of each well, the surface area starts from $650 \times 650 \mu\text{m}^2$ at the bottom of the well and increases up to $1360 \times 1360 \mu\text{m}^2$ at the top.

Standard microfabrication procedures were used to manufacture the nwSlide, as described in detail in ref. 11. Briefly, a low stress nitride (2000 Å) was used as masking material. Contact lithography was performed using a quartz mask. Nanowells were etched through 500 μm thick silicon wafers (Okmetic) by 30% potassium hydroxide at 70 °C for ≈ 800 min. The nitride was stripped by 50% hydrofluoric acid. The resulting silicon grid wafer was then anodically bonded to a 500 μm borofloat glass wafer (Planoptik), followed by dicing into the nwSlide format.

Bacterial strains and electrocompetent cell preparation

All *E. coli* strains used in the study are listed in Table 1. Bacteria were cultured in either Müller-Hinton II (MHII) (BD, USA) or Luria-Bertani (LB) broth (Sigma Aldrich). All strains were streaked on LB agar plates from glycerol stocks stored at -80 °C, and grown at 37 °C for 18 h before use. Electrocompetent cells were either purchased from Invitrogen, USA (MegaX DH10B™ T1^R) or prepared by diluting an overnight *E. coli* W3110 culture in LB 1:100 in 25 ml LB, which was



Fig. 1 General workflow for selection and high-resolution phenotypic screening of bacterial mutants in the nwSlide. (a) FACS-based selection and sorting of single bacterial mutants in individual nanowells of the nwSlide, pre-filled with 500 nl of growth medium each. (b) While bacteria proliferate during incubation on the slide, absorbance (black dashed arrow) and fluorescence (red dashed arrow) are recorded at frequent intervals. Absorbance data are processed with the nanoculture optical signal analysis tool (nOSAT) to obtain the growth profile of each nanoculture. Fluorescence recordings in combination with a fluorescent substrate can identify mutants with decreased or increased enzymatic activity. (c) Guided by the nanowell identification number, bacteria showing the desired phenotype, based on growth profile, enzymatic activity or morphotype, are retrieved from the nwSlide (d) and subcultured in a larger-scale format to enable genotypic analysis and subsequent storage.



Table 1 Bacterial strains used in this study

Strain	Genotype	Ref.
W3110	<i>E. coli</i> K-12 F- λ - <i>rph-1</i> <i>INV(rrnD, rrnE)</i>	17
JW1909	BW25113 Δ <i>fliD::kan</i>	NBRP (NIG, Japan): <i>E. coli</i>
JW1910	BW25113 Δ <i>fliS::kan</i>	NBRP (NIG, Japan): <i>E. coli</i>
JW1911	BW25113 Δ <i>fliT::kan</i>	NBRP (NIG, Japan): <i>E. coli</i>
ARD219	W3110 <i>cyaA::Tn5</i>	This work
ARD220	W3110 <i>lacZ::Tn5</i>	This work
ARD230	W3110 <i>envC::Tn5</i>	This work
ARD232	W3110 <i>rodZ::Tn5</i>	This work
MegaX DH10B TM T1 ^R	<i>E. coli</i> DH10B TM	Invitrogen, USA
D18	<i>E. coli</i> DH10B TM <i>tnpX::TnMHA</i>	This work
D40	<i>E. coli</i> DH10B TM <i>yebB::TnMHA</i>	This work
L43	<i>E. coli</i> DH10B TM <i>yhgE::TnMHA</i>	This work
B5	<i>E. coli</i> DH10B TM <i>recF::TnMHA</i>	This work
G13	<i>E. coli</i> DH10B TM <i>mocA::TnMHA</i>	This work
A4	<i>E. coli</i> DH10B TM <i>rfaJ::TnMHA</i>	This work
D14	<i>E. coli</i> DH10B TM <i>casE::TnMHA</i>	This work

grown to OD₆₀₀ \approx 0.4. Bacteria were concentrated 100-fold, washed 3 times with ice-cold MiliQ water and stored in 25 μ l aliquots at -80°C until use.

Construction of pMHA transposon vector

The FRT-flanked kanamycin cassette was PCR-amplified from pKD4 with the SacI-Kan-FP and KpnI-Kan-RP primers to introduce SacI and KpnI restriction sites, using Phusion High-Fidelity (PHF) DNA polymerase. The PCR-amplified kanamycin cassette was purified with illustraTM GFXTM PCR and Gel Purification kit (GE Healthcare, UK) according to the manufacturer's instructions. The pMOD-2 Vector (Epicentre, USA) was isolated from an overnight *E. coli* W3110 culture in LB broth supplemented with 100 $\mu\text{g ml}^{-1}$ ampicillin. The PCR-amplified kanamycin cassette and pMOD-2 were digested with SacI-HF and KpnI-HF, mixed at 1:2 ratio (vector:insert), and ligated with T4 DNA ligase at 16°C overnight to construct pMOD-2-KAN. Electrocompetent *E. coli* W3110 cells were electroporated with 5 μ l of the ligation reaction. Electroporated bacteria were recovered in 1 ml SOC broth for 2 h at 37°C , with shaking at 200 r.p.m., then plated on LB agar plates supplemented with 50 $\mu\text{g ml}^{-1}$ kanamycin and incubated overnight at 37°C . Colonies transformed with pMOD-2-KAN were transferred in LB broth with 50 $\mu\text{g ml}^{-1}$ kanamycin and incubated overnight at 37°C . Overnight cultures were pelleted and pMOD2-KAN was isolated using the MiniPrep kit (Qiagen, Germany) according to manufacturer's instructions. To clone a GFP-expressing gene in pMOD2-KAN, *gfpmut2* and its IPTG-inducible promoter were PCR-amplified from pKEN1-GFPmut2 with SalI-GFP-FP and HindIII-GFP-RV primers using PHF DNA polymerase, and purified as described above. The PCR-amplified *gfpmut2* and pMOD-2-KAN were digested with SalI-HF and HindIII-HF, and ligated as described above to construct vector pMOD-2-KAN-GFPmut2, hereafter named as pMHA. Electroporation of pMHA into *E. coli* W3110, transformant selection and plasmid isolation was performed as described above.

Transposon mutagenesis

Transposon libraries using the custom-made transposon TnMHA were prepared by linearizing pMHA with ScaI-HF, and by PCR-amplifying the TnMHA sequence with PHF DNA polymerase using primers ME Plus 9-3' and ME Plus 9-5', followed by PCR purification in TE buffer as described above. The TnMHA transposon was prepared by mixing 2 μ l of TnMHA amplicon (100 ng μl^{-1}), 4 μ l EZ-Tn5 transposase (Epicentre), and 2 μ l glycerol, followed by incubation at RT for 30 min. 1 μ l of the TnMHA transposon was electroporated in 40 μ l MegaX DH10BTM T1^R electrocompetent cells according to the manufacturer's instructions. After electroporation, 1 ml SOC medium was added and bacteria were incubated for 2 h at 37°C . Bacteria were then diluted to 5 ml SOC supplemented with 50 $\mu\text{g ml}^{-1}$ kanamycin and 1 mM IPTG and incubated overnight at 37°C , under shaking conditions. The overnight culture containing TnMHA mutants was then single-sorted on a nwslide with FACS as described below.

Strains ARD219, ARD220, ARD230, and ARD232 were constructed using the EZ-Tn5 <KAN-2> Tnp transposome kit (Epicentre) according to the manufacturer's instructions using electrocompetent *E. coli* W3110.

FACS of bacteria on the nwslide

Sorting was performed in a BD InfluxTM cell sorter fitted with a 100 μm nozzle. Sheath fluid and sample pressure, amplitude and frequency were calibrated for small particle sorting using beads between 0.22–1.34 μm (SPHEROTM Flow Cytometry Nano Fluorescent Size Standard Kit, Spherotech, USA). Sheath fluid was autoclaved and filtered with a 0.2 μm filter to ensure it is sterile and particle-free. Forward scatter (FSC) and side scatter (SSC) parameters were adjusted so that the calibration beads are on scale in FSC-W vs. FSC-H and SSC-W vs. SSC-H plots. This enabled us to detect bacteria based on their size, without additional labeling. To prepare bacteria for FACS, overnight cultures were subcultured in fresh media and incubated at 37°C under shaking at 200 r.p.m. until



Right before sorting bacteria, nwSlides were filled with LB or MHII broth by manually spreading a total volume of ≈ 500 μ l broth in a single pipetting step, under sterile conditions. Events in selected gates were then sorted in the pre-filled nwSlides. When mixed samples of wt *E. coli* W3110, and strains ARD219, ARD220, ARD230, ARD232 were sorted, MHII broth was supplemented with 10 mM of 4-methylumbelliferyl β -D-galactopyranoside (MUG). When sorting the TnMHA transposon library, MHII broth was supplemented with 50 μ g ml^{-1} kanamycin and 1 mM IPTG. Directly after sorting, the nwSlide was sealed to prevent evaporation with a sterile polyester acrylate membrane (Thermo Fisher Scientific, USA). The porosity of this membrane enables gas exchange to sustain cell culture and its transparency is compatible with microscopy and spectrophotometry.

Growth parameters were assessed based on spectrophotometric measurements and subsequent data analysis. nwSlides inoculated with single bacteria *via* FACS were placed in a custom-designed microtiter plate adaptor as previously described,¹³ and incubated for 16 h at 37 °C in an Infinite® M1000 PRO plate reader (TECAN, Switzerland) with OD₆₀₀ measured every 30 min. The baseline OD₆₀₀ was subtracted from all OD₆₀₀ kinetic recordings, which is defined as the minimum absorbance recorded in the first 8 kinetic recordings. Then, the OD₆₀₀ recordings were processed with the nanoculture Optical Signal Analysis Tool (nOSAT) to select for nanowells positive for growth and to calculate growth parameters (T_{lag} , growth efficiency and OD_{max}). A detailed explanation of this algorithm can be found in Note S2† and in Fig. S3.†

To prepare mixed cultures, equal ratios of ARD219, ARD230, ARD232 and wt *E. coli* were resuspended in PBS. Then, the *lacZ*::Tn5 mutant was added to these mixed cultures at a 20% (Mix_{20%}), 2% (Mix_{2%}) and 0.2% (Mix_{0.2%}) representation. Mixed cultures were screened in the presence of MUG and spectrophotometric data were processed as described above. To screen for mutants with inactive β -galactosidase, the RFU_{max} values of all nanocultures were plotted and mutants with RFU_{max} below the phenotypic discrimination threshold (1878 RFU), defined by ARD220, were marked as potential mutants.

Bacteria grown on the nwlSlide were retrieved for genotypic screening by piercing the membrane of the nanowell containing bacteria with a 26G 1/2" needle (BD) or 30G 1/2", 0.45 × 13 mm needle (Terumo, USA) attached to a 5 or 1 ml syringe (BD). Then the needle was dipped in 100 µl of broth in a 1.5 ml microcentrifuge tube, which was incubated overnight at 37 °C shaking at 200 r.p.m. For sample storage, we plated the overnight culture in LB agar plates to obtain single colonies and prepare glycerol stocks. For genotypic screening, cultures were pelleted and resuspended in 100 µl sterile MiliQ water. Bacteria were lysed by heating at 95 °C for 10 min. To verify whether cultures derived from one, two or three different flagellar mutants, PCR reactions were prepared using illustraTaq Beads (GE Healthcare) by adding 1 µl of the bacterial lysates, 1 µl of Kan-FP and fliT-RP primers and MiliQ water to a total volume of 25 µl. To verify whether bacteria were wt or mutants for *lacZ*, PCR reactions were prepared using illustraTaq Beads by adding 1 µl of the bacterial

Lab Chip, 2018, **18**, 1767–1777 | 1771

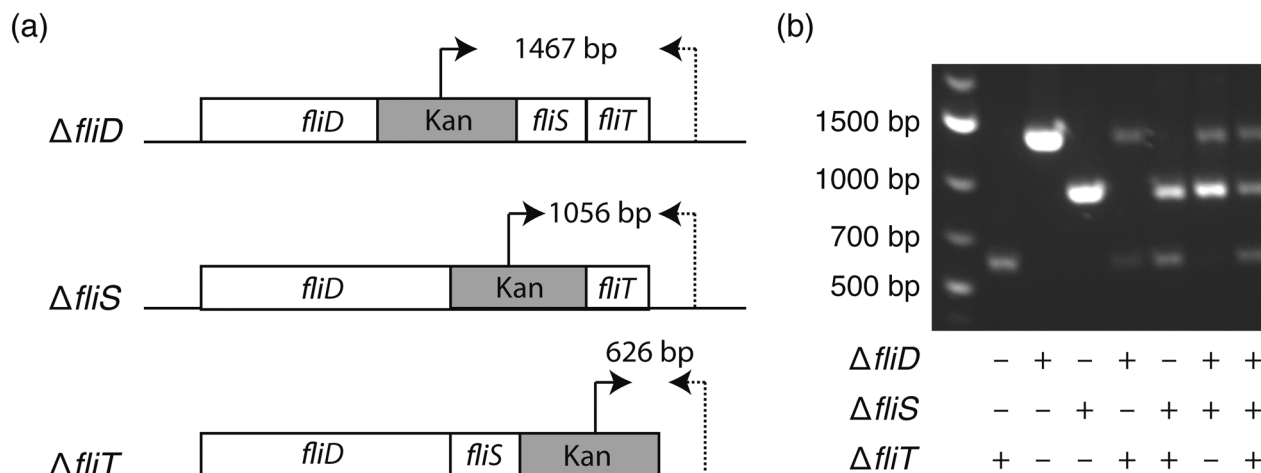


Fig. 2 Genetic construction of flagellar mutants. (a) Schematic representation of the flagellar mutants $\Delta fliD$, $\Delta fliS$, and $\Delta fliT$ in strain W3110, with annealing sites of primers Kan-FP (arrow) and fliT-RP (dotted arrow) shown. The size of their respective PCR product, indicated in base pairs (bp), is used to differentiate the three mutants from each other. (b) The expected size of PCR bands generated by primers Kan-FP and fliT-RP in mono-clonal and mixed cultures as indicated shows the feasibility of this approach for validating the FACS gating strategy.

recordings and calculating the T_{lag} , which represents the exact time point when a bacterial culture transitions from lag to logarithmic phase.¹³ The second checkpoint is designed to filter out growth artifacts. This is achieved by analysing maximum absorbance at 600 nm of each nanoculture, which should fall within 0.006–0.075. A culture that fails to reach

the lower limit contains usually no bacteria, whereas those exceeding the higher limit are usually artifacts. The third checkpoint calculates growth efficiency in each nanoculture. The nOSAT algorithm controls that the net absorbance increase of the nanoculture is ≥ 0.006 . This excludes any nanowell containing air bubbles, since their net absorbance increase is usually negative.

To test the specificity and sensitivity of nOSAT, we used absorbance data from the wild type (wt) *E. coli* strain W3110 (Table 1). The bacterial cultures were single-sorted onto nwSlides, then incubated for 16 h at 37 °C in a plate reader. Bacterial growth of each nanowell was monitored by OD₆₀₀ readings every 30 min. Absorbance data from 997 randomly selected nanowells from three independent experiments were processed with nOSAT, which identified 644 nanowells as positive and 353 as negative for growth. To confirm these results, we examined the same 997 nanowells by phase contrast microscopy. A comparison of the nOSAT results with the microscopy observations showed 640 nanowells true positives for growth, 321 true negatives, 4 false positives and 32 false negatives. Based on these results, we determined the sensitivity of nOSAT to be 95.24% with a 95% confidence interval (C.I.) of 93.34–96.72%. The specificity was 98.77% with a 95% C.I. of 96.88–99.66%.

Overall, nOSAT enables rapid identification of the growth profile of each nanoculture and in parallel, extracts information about growth efficiency and the duration of the lag phase (T_{lag}). The latter is of particular interest when considering that a single bacterium is used as inoculum in each nanoculture. Starting with an identical inoculum allows precise comparisons of growth between bacterial cultures.

Phenotypic screening of bacterial nanocultures

The ability to synchronously initiate hundreds of bacterial cultures with one bacterium each and monitor their growth profiles by optical recordings prompted us to exploit the

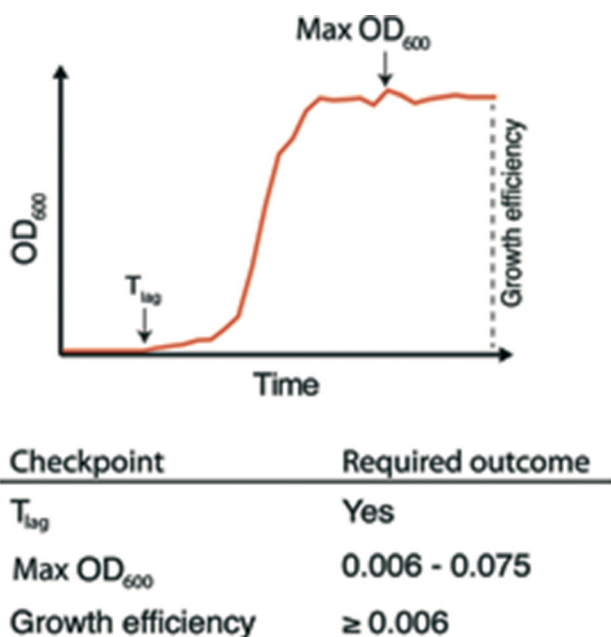


Fig. 3 Schematic representation of checkpoints forming the basis of the nOSAT algorithm. During incubation, optical recordings from each nanoculture are processed and controlled for three checkpoints with the nOSAT algorithm. Generation of T_{lag} represents the first checkpoint, which controls whether a nanoculture has transitioned from lag to log phase. The second checkpoint controls whether maximum OD (OD_{max}) is ranging within 0.006–0.075. The third checkpoint controls whether growth efficiency is ≥ 0.006 . If a nanoculture passes all 3 checkpoints, then it is considered as positive for bacterial growth.



nwSlide as a novel tool for high throughput analysis in microbiological research. Phenotypic screening is a method used to identify a strain with a specific phenotypic trait and isolate it from the thousands of mutants present in a mutagenized bacterial culture. Traditionally, phenotypic screening is a step-wise process where individual mutants are first isolated as bacterial colonies on selective agar plates. A quantitative phenotypic analysis is then performed; subculturing of monoclonal bacteria in microtiter plates, sometimes in the presence of colorimetric or fluorometric substrates, enables monitoring of bacterial growth and phenotype in parallel by spectrophotometry.

With an ultimate goal of developing a one-step process for simultaneous selection and phenotypic screening in the monoclonal liquid nanocultures, we first designed a phenotypic assay aimed to discriminate between positive and negative β -galactosidase (β -gal) phenotypes using the wt *E. coli* strain and a *lacZ*::Tn5 mutant (strains W3110 and ARD220, Table 1). Expression of β -gal enables wt *E. coli* to hydrolyse the substrate 4-methylumbelliferyl β -D-galactopyranoside (MUG), which in hydrolysed form emits fluorescence at 450 nm. In contrast, the *lacZ*::Tn5 mutant is unable to hydrolyse

MUG. To define the basal levels of MUG hydrolysis in each strain, we cultured bacteria in the presence of MUG on two nwSlides for each strain. During the 16 h incubation at 37 °C, bacterial growth was monitored in each nanowell at OD₆₀₀ and MUG hydrolysis at OD₄₅₀ every 30 min. Processing of the OD₆₀₀ recordings with nOSAT identified 1161 nanowells with growth for the wt *E. coli* and 1257 nanowells with growth for the *lacZ*::Tn5 mutant. To define the range of fluorescence intensity expected from MUG hydrolysis, we plotted the RFU_{max} values from each nanowell with bacterial growth. Fig. 4a shows a wide distribution of RFU_{max} for the wt *E. coli*, with the 1st percentile at 4638 RFU and the 99th percentile at 21 833 RFU. Nanocultures with the *lacZ*::Tn5 mutant show, as expected, much lower RFU_{max} and a narrow distribution with the 1st percentile at 766.6 RFU and the 99th percentile at 1878 RFU. Close inspection reveals a very minor overlap between the RFU_{max} distribution of the two strains, with only two wt *E. coli* nanocultures appearing below the 99th percentile of the *lacZ*::Tn5 mutant distribution (Fig. 4b). Based on these results, we defined the 99th percentile of the *lacZ*::Tn5 mutant (1878 RFU) as the fluorescence threshold to discriminate between positive and negative β -gal phenotypes.

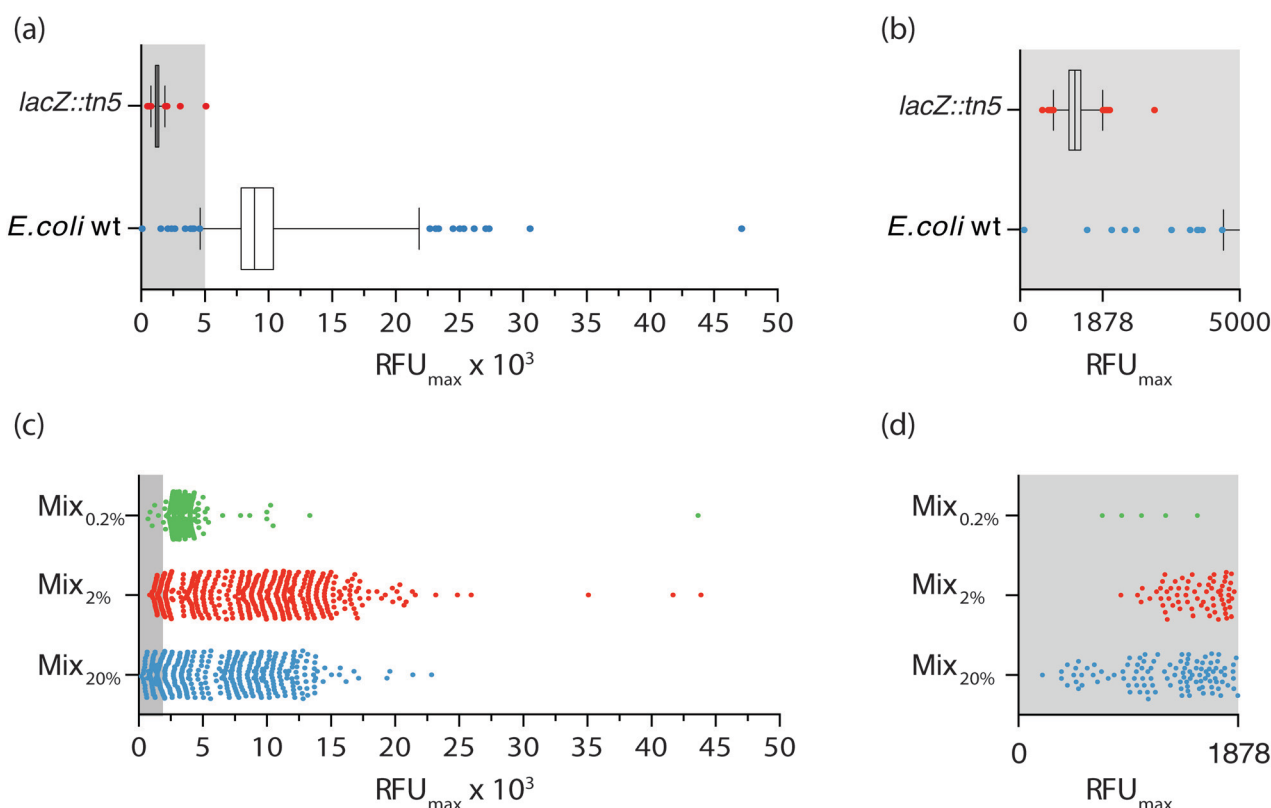


Fig. 4 Phenotypic screening to detect mutants with impaired β -galactosidase activity. (a) Distribution of RFU_{max} from nanowells inoculated with *E. coli* W3110 wt and the *lacZ*::Tn5 mutant. Data is pooled from two biological replicates, representing 1161 (*E. coli* W3110 wt) and 1257 (*lacZ*::Tn5 mutant) nanocultures. Whiskers define 1st and 99th percentile. (b) Magnification of data in the range 0–5000 RFU_{max} from panel (a), showing in greater detail the narrow RFU_{max} distribution of *lacZ*::Tn5 mutant nanocultures, and their minor overlap with the *E. coli* W3110 wt. (c) Distribution of RFU_{max} from nanowells inoculated with single bacteria from mixed cultures containing equal ratio of strains *E. coli* W3110 wt, ARD219, ARD230 and ARD232 that are all positive for *lacZ*, as well as 20% (Mix_{20%}), 2% (Mix_{2%}) and 0.2% (Mix_{0.2%}) of the *lacZ*::Tn5 mutant strain. Data originate from one biological replicate. (d) Magnification of data in the range 0–1878 RFU_{max} from panel (c), showing in greater detail the number of mutants with RFU_{max} below the phenotypic discrimination threshold in each Mix.

Having shown that the FACS-linked nwSlide works excellently to generate monoclonal nanocultures for phenotypic screening, we next extended this method to develop a one-step pro-

The dual-selection transposon was next used to generate TnMHA mutants. PCR-amplified TnMHA mixed with EZ-Tn5 transposase was electroporated in *E. coli* cells (MegaX DH10B™ T1^R, Table 1), and bacteria were allowed to recover during a 2 h incubation. This procedure typically generates 1×10^5 transposon mutants, which constitute $\leq 0.002\%$ of the total bacterial population. As this low number classifies the mutant cells as rare events for FACS, we enriched for mutants in the bacterial culture by overnight incubation in SOC medium supplemented with kanamycin. Moreover, IPTG was added to maximize bacterial expression of GFP for subsequent fluorescence sorting. The bacterial culture was loaded onto the FACS instrument, where the GFP negative gate had been previously set using non-transformed *E. coli* as a negative control. The GFP vs. FSC-H plot showed that the GFP positive fraction was 10.9% of the total sample (Fig. 5b). This indicated a successful generation and enrichment for TnMHA mutants. To isolate and subculture the individual mutants, we single-sorted the GFP positive bacteria on a nwSlide pre-filled with Müller-Hinton medium with kanamycin. After overnight incubation with OD₆₀₀ recordings, data processing by nOSAT identified 371 nanocultures with TnMHA mutants. This shows that TnMHA successfully enables fluorescence-based selection of transposon mutants in the FACS-linked nwSlide system. A recovery rate of 56% (371 mutants out of 672 nanowells) suggests that a number of wt cells also were FACS sorted onto the nwSlide, but as they were exposed to medium containing kanamycin, they were unable to grow. A more stringent gating strategy for GFP⁺ mutant selection in the FACS instrument would increase the recovery of transposon mutants.



Fig. 5 Design of TnMHA to enable FACS-based selection and phenotypic screening of transposon mutants in the nwSlide (a) schematic representation of the transposon TnMHA, which provides dual selection based on GFP fluorescence (*gfpmut2*) and kanamycin resistance (*kan*). ME = mosaic ends, P_{kan} = kanamycin promoter, *srp* = sterically repressed promoter. To enable optional removal of the *kan* gene, it is flanked by flippase recognition target (FRT) sequences. (b) FACS analysis of bacteria electroporated with TnMHA, showing 10.9% mutant cells in the total population. (c and d) Distribution of T_{lag} (c) and growth efficiency (d) of the TnMHA mutants sorted in (b). (e) Phase contrast (upper panel) and confocal fluorescence (lower panel) microscopy of TnMHA mutants in nanowells A4 and D14 show how their morphotypes differ from *E. coli* W3110 wt. Scale bars = 10 μ m (phase contrast microscopy) and 25 μ m (confocal fluorescence microscopy).

Following the dual-selection based on GFP expression during sorting and kanamycin resistance during growth, we screened the 371 TnHMA mutants for a phenotype of interest. As a proof-of-concept, we performed growth phenotyping based on data generated by the nOSAT analysis of the monoclonal nanocultures. When analysing the length of the lag phase, T_{lag} , in the mutant population, we found a median of 9 h (Fig. 5c). By applying the 95th percentile (12 h) as an upper cut-off, we identified 11 mutants with unusually long lag phase. From these, we recovered mutants in nanowells D18, D40 and L43, and mapped the transposon insertion sites using a cloning-free strategy, rapid amplification of transposon ends (RATE), based on single-primer PCR. Sequencing of RATE-generated PCR products revealed transposon insertions in the genes *tnpX* (D18), in *yebB* (D40) and in *yhgE* (L43) (Table 1). Similarly, we applied the 5th percentile (7.5 h) as a lower cut-off to identify mutants with short lag phase (Fig. 5c). Out of 31 mutants, we recovered the mutant with

shortest lag phase (nanowell B5), and located the transposon insertion site in *recF* (Table 1).

As a second approach, we performed phenotypic screening based on the nanocultures' growth efficiency defined by nOSAT. The mutant population showed a median growth efficiency of 0.029 A.U. (Fig. 5d). By applying the 95th percentile (0.039 A.U.) as cut off, we selected the mutant in nanowell G13 as it showed increased growth efficiencies (0.052 A.U.), and recovered bacteria for subsequent RATE analysis. Sequencing of RATE-generated PCR products located the transposon insertion site at *mocA*. Taken together, our experiments demonstrate that the FACS-linked nwSlide provide a novel method to identify potential new roles for genes based on multiple parameter analysis that could otherwise go unnoticed. Further work, however, would be required to unravel the link between gene function and the phenotypes discovered, but this falls outside the scope of the present investigation.



Conclusions

Merging the nwSlide with FACS and spectrophotometry greatly shortens the time for selection and screening protocols. Plating of bacterial cultures on selective agar plates, isolation of monoclonal colonies the following day, and subcultivation in liquid medium for screening purposes can now be omitted. The FACS-linked nwSlide allows up to 672 single bacteria to be sorted in individual wells in 15 min. Placement of the inoculated nwSlide in a temperature-controlled plate reader enables immediate spectrophotometric monitoring of growth and phenotypic screening. The nOSAT algorithm, specifically developed for efficient handling of large amount of

The versatility and modular workflow provide easy adaptation of the nwSlide to a wide range of laboratory settings. Its use in basic research laboratories can be readily extended to industrial and clinical laboratories, where novel applications, such as pathogen surveillance, can be addressed by high-throughput phenotypic screening of clinical or environmental samples. By reinventing traditional microbiology assays in

miniaturized formats, the output of bacterial culturing and phenotypic screening in diverse environments can be greatly increased.

Author contributions

H. A., E. W., H. A. S., and A. R.-D. conceived the presented idea. H. A. and E. W. performed a preliminary investigation to test the feasibility of the project. H. A. and M. V. G. designed and carried out all experiments. H. A. designed and applied the analysis algorithm on generated data. A. R.-D. and H. A. S. supervised the project and contributed to result interpretation. H. A., M. V. G., and A. R.-D. wrote the manuscript and E. W. and H. A. S. provided critical feedback.

Conflicts of interest

There are no conflicts to declare.

Acknowledgements

We thank Dr. J. Mikes at the National Mass Cytometry Facility at ScilifeLab, Stockholm, for his help in optimizing FACS. This work was supported by grants from the Swedish Research Council, Stockholm County Council (ALF project), European Research Council under the European Union's Seventh Framework Programme (FP/2007-2013)/ERC Grant Agreement No. 615458.

Notes and references

- 1 R. J. Petri, *Cent. für bacteriologie und Parasitenkd.*, 1887, vol. 1, pp. 279–280.
- 2 W. Hesse, *ASM News*, 1992, 58, 425–428.
- 3 C. Ingham and P. M. Schneeberger, in *The Role of New Technologies in Medical Microbiological Research and*

Diagnosis, ed. J. P. Hays and W. B. Leeuwen, Bentham e Books, Rotterdam, 2012, pp. 3–15.

- 4 M. Y. Galperin and E. V. Koonin, *Trends Biotechnol.*, 2010, 28, 398–406.
- 5 A. Blomberg, *Curr. Opin. Biotechnol.*, 2011, 22, 94–102.
- 6 J. Warringer, E. Ericson, L. Fernandez, O. Nerman and A. Blomberg, *Proc. Natl. Acad. Sci. U. S. A.*, 2003, 100, 15724–15729.
- 7 J. Warringer, D. Anevski, B. Liu and A. Blomberg, *BMC Chem. Biol.*, 2008, 8, 3.
- 8 R. Martinez and U. Schwaneberg, *Biol. Res.*, 2013, 46, 395–405.
- 9 M. Zackrisson, J. Hallin, L.-G. Ottosson, P. Dahl, E. Fernandez-Parada, E. Ländström, L. Fernandez-Ricaud, P. Kaferle, A. Skyman, S. Stenberg, S. Omholt, U. Petrovič, J. Warringer and A. Blomberg, *G3: Genes, Genomes, Genet.*, 2016, 6, 3003–3014.
- 10 Y. Qiao, X. Zhao, J. Zhu, R. Tu, L. Dong, L. Wang, Z. Dong, Q. Wang and W. Du, *Lab Chip*, 2018, 8, 62.
- 11 S. Lindström, R. Larsson and H. A. Svahn, *Electrophoresis*, 2008, 29, 1219–1227.
- 12 S. Lindström and H. Andersson-Svahn, *Biochim. Biophys. Acta, Gen. Subj.*, 2011, 1810, 308–316.
- 13 E. Weibull, H. Antypas, P. Kjäll, A. Brauner, H. Andersson-Svahn and A. Richter-Dahlfors, *J. Clin. Microbiol.*, 2014, 52, 3310–3317.
- 14 S. Lindström, M. Eriksson, T. Vazin, J. Sandberg, J. Lundeberg, J. Frisén and H. Andersson-Svahn, *PLoS One*, 2009, 4, 1–9.
- 15 S. Lindstrom, M. Hammond, H. Brismar, H. Andersson-Svahn and A. Ahmadian, *Lab Chip*, 2009, 9, 3465–3471.
- 16 A. Karlyshev and M. J. Pallen, *BioTechniques*, 2000, 28, 1078–1082.
- 17 M. Karow and C. Georgopoulos, *J. Bacteriol.*, 1992, 174, 702–710.

